Frictional behavior of materials in the 3D SAFOD volume

B. M. Carpenter,[1] C. Marone,[1] and D. M. Saffer[1]

Received 13 November 2008; revised 17 January 2009; accepted 23 January 2009; published 7 March 2009.

[1] We report on frictional properties of rocks within the 3-D crustal volume surrounding the San Andreas Fault Observatory at Depth (SAFOD). Samples include lithologies adjacent to the San Andreas Fault (SAF) in the subsurface, SAFOD borehole rocks, and synthetic fault gouge composed of talc, serpentinite, and quartz. Granodiorite, arkosic sandstone, and siltstone samples from the SAFOD borehole are frictionally strong ($\mu = 0.56 - 0.66$). Sand and clay-rich lithologies from outcrop exhibit friction in the range $\mu = 0.56 - 0.68$. Natural serpentinite thought to abut the SAF at depth exhibits low friction ($\mu = 0.18 - 0.26$). Our results indicate that 1) serpentinite exhibits low strength, but is not weak enough to completely satisfy weak fault models, 2) all other samples are consistent with a strong fault and crust and, 3) if the SAF is weak ($\mu \leq 0.2$) due to the presence of serpentinite or talc, these minerals would likely need to constitute over 50% by weight of the shear zone.
Citation: Carpenter, B. M., C. Marone, and D. M. Saffer (2009), Frictional behavior of materials in the 3D SAFOD volume, *Geophys. Res. Lett.*, *36*, L05302, doi:10.1029/2008GL036660.

1. Introduction

[2] A central problem in evaluating the relationship between fault zone properties and earthquake physics is a lack of detailed data for fault zone materials recovered from hypocentral depths. The SAFOD borehole near Parkfield, California provides unprecedented access to wall rock and fault core materials from depths to 3 km; one goal of the SAFOD project was to return samples for laboratory study [*Hickman et al.*, 2004]. In 2004 and 2005, the SAFOD Main Hole penetrated two strands of the actively creeping San Andreas Fault [*Hickman et al.*, 2005, 2007], and returned cuttings with a spatial resolution of ~3 m. Together with core and cuttings recovered in SAFOD Phase III drilling, these samples provide new insights on fault zone architecture and composition.

[3] To date, SAFOD and related studies have provided data on fault zone and wall rock lithologies [*Solum et al.*, 2006], stress orientations [*Hickman and Zoback*, 2004], and frictional strength [*Tembe et al.*, 2006; *Morrow et al.*, 2007]. These data will help to resolve: 1) debate concerning the absolute strength of the San Andreas Fault [e.g., *Scholz*, 2000; *Hardebeck and Michael*, 2004] and 2) controls on the stability of frictional sliding. However, at present, frictional strength and constitutive properties of materials within the fault zone and crust surrounding SAFOD are not well known because only a limited number of laboratory studies have been completed [e.g., *Tembe et al.*, 2006; *Kopf*, 2007]. Furthermore, the SAFOD borehole penetrates only a limited number of lithologies that abut the fault. Here, we document frictional strength and constitutive behavior, via laboratory shearing measurements on cuttings and outcrop samples that cover a wide range of lithologies abutting the San Andreas Fault and surrounding the SAFOD borehole.

2. Experimental Samples

[4] We collected outcrop samples of lithologies thought to comprise and abut the fault zone at depth, on the basis of: 1) detailed geologic cross-sections for the SAFOD sites [*Thayer and Arrowsmith*, 2005; *Arrowsmith et al.*, 2005] (Figure 1a), 2) published geologic maps [*Dibblee*, 1973; *Sims*, 1988; *Thayer et al.*, 2004], and 3) cuttings retrieved during SAFOD phase I and phase II drilling (Figure 1a). We selected the outcrop sampling locations using detailed geologic maps of the Cholame Valley and Cholame Hills quadrangles [*Dibblee*, 1973], the Carrizo Plain, Caliente, and La Plaza Ranges regions [*Sims*, 1988], and Middle Mountain [*Thayer et al.*, 2004]. Sample sites are shown on Figure 1b. One key focus of our sampling campaign was to obtain natural serpentinite from around the New Idria Mine, which is considered equivalent to serpentinite that abuts the creeping section of the San Andreas Fault in central CA and has been hypothesized to cause both its mechanical weakness and aseismic behavior [*Irwin and Barnes*, 1975]. XRD analysis on the serpentinite sample indicates that it is comprised of ~90% lizardite and ~10% hydrotalcite.

[5] Experiments performed on outcrop samples provide constraints on the frictional behavior of host rock and fault gouge derived from rocks surrounding the SAF, many of which were not sampled by the SAFOD boreholes (Figure 1). In addition, we obtained cuttings from phases I and II of SAFOD drilling. These include granodiorite recovered at a measured depth (MD) of 1463 m (total vertical depth (TVD) of ~1.5 km), arkosic metasandstone (MD = 3063 m and 3065 m; TVD = ~2.4 km), and siltstone (MD = 3990 m; TVD = ~3.1 km) (Figure 1). The granodiorite and arkosic metasandstone samples are cuttings from Phase I whereas the siltstone is from the core catcher during Phase II. In order to provide data for end member behavior and insight into the processes controlling frictional behavior, we also conducted experiments on synthetic mixtures of angular quartz sand (US Silica Co. F110, mean grain size 127 μm), talc ($\leq$125 μm), and serpentinite ($\leq$125 μm). The talc was acquired from Ward's Natural Science and was collected from a schist mine in Balmat, NY.

3. Experimental Methods

[6] Rock and core samples were crushed in a roll crusher with a wheel separation of 2 mm and then further pulverized

[1]Department of Geosciences and Energy Institute Center for Geomechanics, Geofluids, and Geohazards, Pennsylvania State University, University Park, Pennsylvania, USA.

0094-8276/09/2008GL036660$05.00

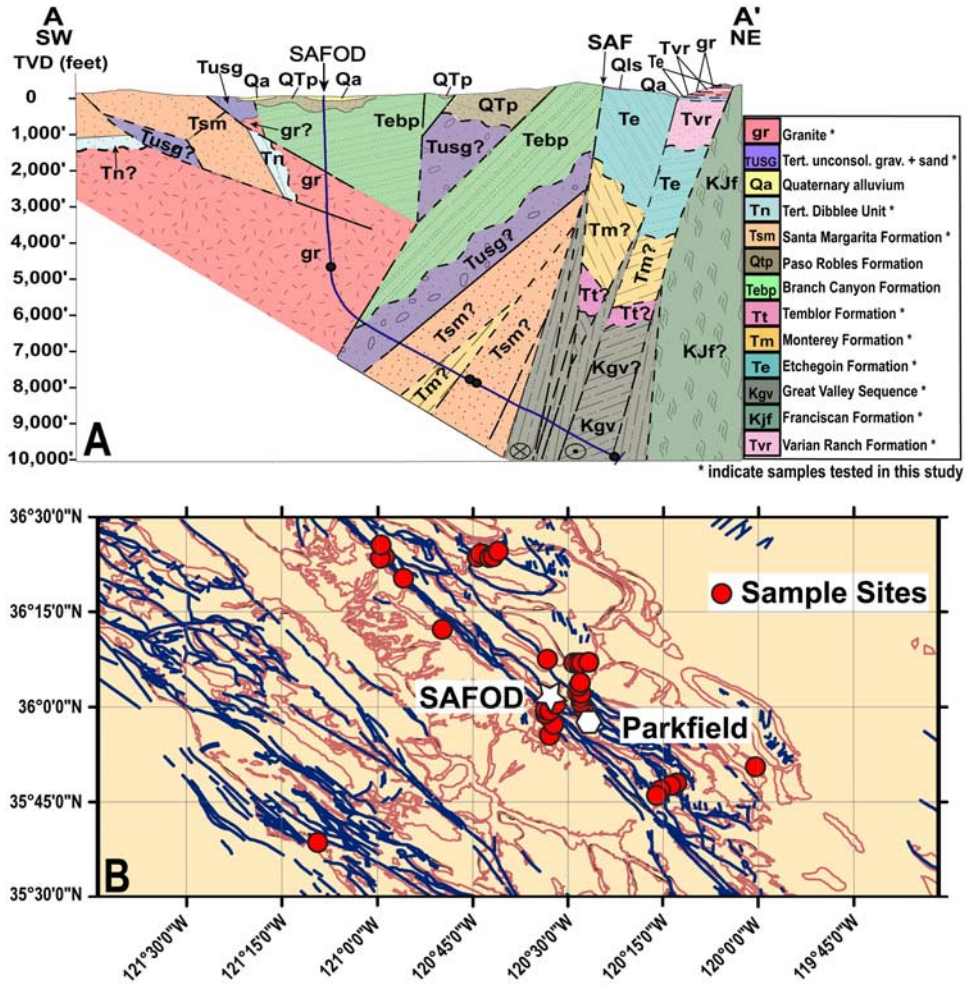

Figure 1. (a) (Color Online) Geologic cross section at the SAFOD borehole [*Thayer et al.*, 2004; *Arrowsmith et al.*, 2005]. Black circles indicate location of cuttings used in this study. (b) Location of outcrop samples (red circles) on topographic (pink lines) base map with faults (dark blue lines) as compiled by Dibblee. A-A′ is perpendicular to the fault trace and crosses the fault at the SAFOD site (white star).

in a shatter box. We removed any metal filings and sieved samples to a grain size of $\leq$125 μm, which allowed for simple, direct comparison with synthetic mixtures in the same size range and with previous work on SAFOD samples, in which samples were ground and sieved to $\leq$149 μm [*Tembe et al.*, 2006]. We sheared samples in layers 3 to 5 mm thick constructed by pouring and smoothing the experimental gouge onto grooved, steel forcing blocks.

[7] We conducted shearing experiments in double direct shear, under both room humidity and controlled pore fluid pressure in a true-triaxial pressure vessel. In this configuration, two gouge layers are sheared simultaneously [e.g., *Ikari et al.*, 2007], and symmetry of the experimental configuration ensures that stresses are the same on each layer and the nominal contact area remains constant (at 0.025 m^2) during shear. Constant normal stress is applied and maintained by a hydraulic servo-control system. Shear occurs by displacing the center block between the two stationary side blocks (Figure 2a). Forces are measured with strain gauge load cells to ±5 N, and vertical and horizontal displacements are measured by DCDTs to ±0.1 μm. We recorded all data continuously at 10 kHz and averaged to values ranging from 1Hz to 1 kHz, depending on shearing velocity.

[8] We began all experiments with a 5 mm shear displacement 'run-in' (Figure 2) to establish a stable shear fabric in the layer and to attain steady-state friction. Detailed friction measurements, including velocity stepping, began after an additional run-in (Figure 2b). We used a normal stress stepping procedure to evaluate the Coulomb failure envelope and friction constitutive properties under a variety of stresses (Figure 2). In our experiments at room temperature and humidity, we investigated normal stresses from 4 to 100 MPa; for experiments under saturated conditions in the pressure vessel with pore (5MPa) and confining (6MPa) pressures applied, we investigated effective normal stresses from 5 to 20 MPa.

[9] We report steady-state sliding friction as the ratio of shear stress to effective normal stress (i.e., assuming zero cohesion for the granular layers), at a load point velocity of 10 μm/s. At each normal stress, the values were obtained after friction reached steady-state, typically at displacements >2.5 mm. Velocity stepping tests were conducted

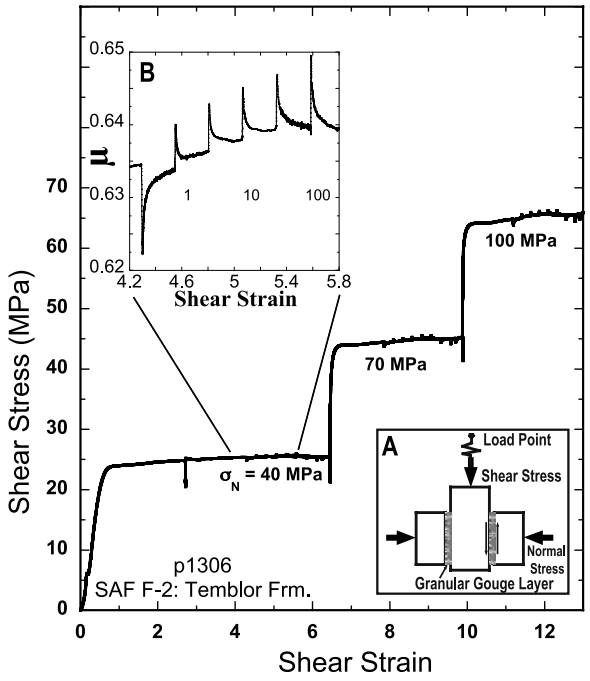

Figure 2. Stress strain curve for a complete, representative experiment. Velocity step tests are performed at each normal stress. Sample SAF F-2 is a Temblor Frm. Sandstone. (a) Schematic showing the sample configuration. The two side blocks are held in place while the center block is driven downward at a constant velocity. The side blocks are allowed to move in the direction normal to the shear direction. (b) Velocity steps; 1–3–10–30–100–300 μm/s. Shear strain is calculated by integrating increments of shear displacement, at the layer boundary, divided by the instantaneous layer thickness. Shear strain and layer thickness refer to one layer of the double-direct shear configuration.

at each normal stress at velocities from 1 to 300 μm/s (Figure 2b). The samples exhibit slip-rate and history-dependent friction behavior consistent with previous studies [e.g., *Marone*, 1998; *Saffer and Marone*, 2003]. Positive values of the friction-rate parameter, $a\text{-}b = \Delta\mu_{ss}/\Delta lnV$, indicate an increase in steady-state friction with increasing velocity (termed velocity strengthening behavior) and negative values of $a\text{-}b$ indicate a decrease in friction with velocity (termed velocity weakening).

4. Results

[10] SAFOD borehole cuttings exhibit consistent coefficients of friction ranging from 0.56 to 0.66; granodiorite (μ = 0.60–0.64) and siltstone (μ = 0.63–0.65) samples are slightly stronger than the two arkosic metasandstone samples (μ = 0.57–0.66 and 0.56–0.65) (Figure 3a and Data Set S1).[1] These values are broadly consistent with the friction coefficients (granodiorite: ~0.65, arkosic metasandstone: ~0.65, and siltstone: ~0.55) reported from previous work on SAFOD cuttings from equivalent measured depths and the same lithologies sheared in a triaxial geometry [*Tembe et al.*, 2006; *Morrow et al.*, 2007]. In contrast, previous experiments on inferred gouge material from SAFOD have yielded coefficients of friction as low as 0.25–0.30 for cuttings [*Kopf*, 2007], 0.40–0.55 for mixtures of sidewall core and cuttings [*Tembe et al.*, 2006], and 0.30–0.50 and 0.40–0.45 for cuttings separates of clay and serpentinite grains with slickensides, respectively [*Morrow et al.*, 2007]. It is important to note that the SAFOD samples used in our study were taken from wall rock and would not be expected to exhibit friction values as low as those reported for gouge from shear zones.

[11] The full range of SAFOD outcrop lithologies we tested are characterized by friction coefficients ranging from μ = 0.56 to 0.68 (Figure 3a and Data Set S1). In contrast, serpentinite from the New Idria region exhibits low fric-

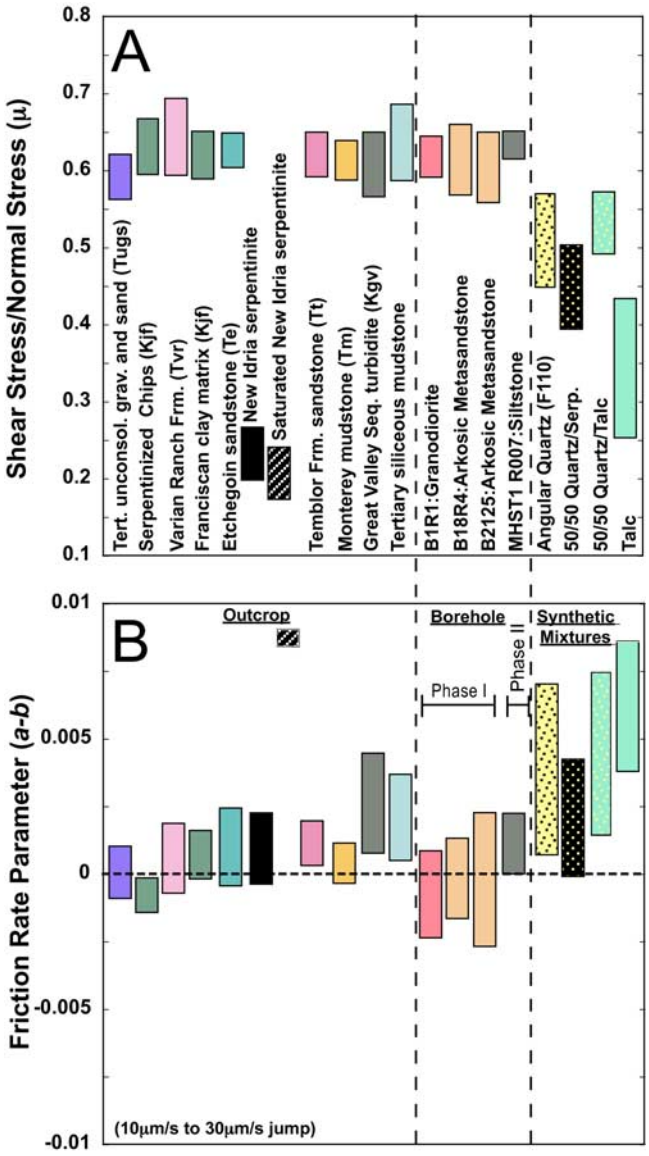

Figure 3. (Color Online) Summary plot showing (a) frictional strength and (b) velocity dependence of outcrop samples, borehole samples, and synthetic mixtures. Horizontal dashed line indicates velocity-neutral behavior ((a-b) = 0) (Data Set S1).

[1]Auxiliary materials are available at ftp://ftp.agu.org/apend/gl/2008gl036660.

tional strength (μ = 0.20 to 0.26) and weakens further upon water saturation (μ = 0.18–0.24), consistent with previous work on serpentine minerals [*Morrow et al.*, 2000]. Synthetic mixtures of 50 wt% quartz – 50 wt% serpentinite exhibit friction of 0.40–0.50; mixtures of 50 wt% quartz – 50 wt% talc exhibit friction coefficients of 0.50 – 0.57 (Figure 3a). Pure talc exhibits friction in the range 0.25–0.43, in agreement with previous work [e.g., *Escartín et al.*, 2008].

[12] The results of velocity stepping tests are summarized in Figure 3b. Granodiorite exhibits a range of behaviors from velocity weakening to slight velocity strengthening behavior (a-b = −0.0020 to 0.0005), arkosic metasandstones are velocity neutral, with a-b values from −0.0020 to 0.0019, and the siltstone is velocity strengthening (a-b = 0.0001 to 0.0021). Outcrop samples exhibited primarily velocity neutral to velocity strengthening behavior, with a subset of samples exhibiting slight velocity-weakening under some conditions (a-b = −0.0011 to 0.0044). The New Idria serpentinite sample was strongly velocity strengthening (a-b = −0.0002 to 0.0021) and became more velocity strengthening once saturated (a-b = 0.0082). Synthetic mixtures of quartz-talc and quartz-serpentinite, along with pure talc and pure quartz, are velocity strengthening.

5. Discussion and Implications

[13] The apparent low frictional strength of the SAF is poorly understood. The lack of an observable heat flow anomaly near the fault, as expected from frictional heat generation, has been interpreted to indicate that the effective friction coefficient along the SAF is ≤0.2 [*Brune et al.*, 1969; *Sass et al.*, 1997; *Williams et al.*, 2004]. Inferred stress orientations around the fault indicate that the maximum horizontal compressive stress is oriented 70–85° to the SAF in the near field, further suggesting that the SAF is weak relative to the surrounding crust [*Zoback et al.*, 1987].

[14] Our results for outcrop and SAFOD wall rock samples are consistent with models invoking a strong crust (μ = ∼0.6) surrounding the SAF. Even the lowest values of friction coefficient reported for gouge and cuttings from secondary faults sampled by SAFOD drilling [*Tembe et al.*, 2006; *Kopf*, 2007; *Morrow et al.*, 2007] are ∼μ = 0.25 – 0.30. These values are still high compared with the apparent weakness of the SAF, suggesting that relative weakness of the SAF is plausible, even if the overall strength of the surrounding crust is controlled by the failure of these subsidiary shear zones.

[15] Talc and serpentinite found in SAFOD cuttings [*Moore and Rymer*, 2007] have been suggested as possible explanations for the apparent weakness and aseismic character of the San Andreas Fault in central California. Our findings for frictional strength of naturally occurring serpentinite thought to influence the mechanics of the SAF [e.g., *Irwin and Barnes*, 1975] are consistent with the possibility that entrainment of these materials in the fault zone is one part of the explanation for its mechanical weakness, though they are not sufficiently weak to completely explain the inferred effective friction coefficient on the SAF. Our results for New Idria area serpentinite, conducted under saturated and controlled pore pressure conditions (μ = ∼0.23 dry and μ = ∼0.18 wet) are also consistent with previous work on the effect of water saturation on serpentine minerals [*Morrow et al.*, 2000].

[16] Our measured friction coefficients for synthetic mixtures of 0.40–0.57 are considerably higher than predicted by heat flow and directional constraints for the SAF, and suggest that ≥50 wt% talc or serpentinite would be required. However, our measurements were conducted primarily under dry conditions, and it is likely that friction is lower under saturated conditions [e.g., *Morrow et al.*, 2000]. We also expect that friction coefficient would be lower under saturated conditions for the other phyllosilicate samples we studied. Additionally, if serpentinite or talc coatings are formed on grains, as has been observed for some clays [*Schleicher et al.*, 2006], then significant weakening may be possible with less than 50 wt% of these minerals.

[17] Both the presence of serpentinite and the granular properties of fault gouge have been linked to aseismic fault slip [e.g., *Marone and Scholz*, 1988; *Reinen et al.*, 1991]. We document primarily velocity strengthening behavior for clay-rich and serpentine lithologies that are probably most relevant to the SAF itself, which is highly consistent with this model and with previous studies on clays and clay-rich gouge [e.g., *Morrow et al.*, 1992; *Saffer and Marone*, 2003]. Our results for frictional velocity dependence of quartzofeldspathic outcrop samples are consistent with previous work on San Andreas Fault system rock from outcrops adjacent to the Hayward fault, which reported velocity strengthening (a-b = 0.003 to 0.015) for a variety of quartzofeldspathic rock types [*Morrow and Lockner*, 2001].

[18] The lithologies we studied are most relevant to shallow depths where material is likely to be unconsolidated, and where fault behavior is generally aseismic [*Marone and Scholz*, 1988]. Notably, visible inspection of SAFOD Phase III core across the main slipping zone documented a thick, well developed, non-cohesive, and clay-rich gouge zone at ∼3 km vertical depth with a ∼2 inch-thick, sheared serpentinite block. On the basis of our results and those of other studies documenting velocity-strengthening of granular gouge, clays, and serpentine minerals, the nature of this shear zone is consistent with the creeping behavior of the SAF in this region [e.g., *Reinen et al.*, 1991; *Morrow et al.*, 1992; *Saffer and Marone*, 2003]. Nevertheless, we note the possibility that these materials could transition to velocity weakening behavior under different conditions not explored here, such as higher slip rates or hydrothermal conditions.

6. Conclusions

[19] Our borehole samples and nearly all of our outcrop samples exhibit relatively high coefficients of friction. The New Idria serpentinite exhibits low friction and although it may contribute to fault weakness it is unlikely to fully explain the apparent weakness of the SAF. The serpentinite also exhibits velocity strengthening behavior (a-b = −0.0002 to 0.0082), consistent with the idea that this material could, in part, cause creeping behavior along this section of the SAF. Sand and sandstone dominated borehole and outcrop samples tend towards velocity neutral to slightly velocity strengthening behavior (a-b = −0.0020 to 0.0044), whereas clay dominated samples are generally velocity strengthening (a-b = −0.0011 to 0.0033). Experiments on synthetic fault gouge indicate that >50 wt%

serpentinite or talc in the fault zone would be needed to explain the apparent weakness of the SAF, unless their effects of friction are strongly controlled by coatings or films at grain boundaries.

[20] **Acknowledgments.** This work was supported by NSF grants EAR-0545702, EAR-0746192, and OCE-0648331 to CJM and DMS. The authors wish to thank M. Underwood, R. Harris, M. Knuth, D. Marone, and H. Tobin for their assistance with fieldwork. We also wish to thank S. Karner, D. Moore and two anonymous reviewers for their insightful comments, which helped improve this manuscript.

References

Arrowsmith, J. R., ASU Team Members, and M. Rymer (2005), Integrated studies of fault zone structure and earthquake geology along the San Andreas Fault at Parkfield, paper presented at EarthScope National Meeting, EarthScope, Santa Ana Pueblo, N. M.

Brune, J. N., T. L. Henyey, and R. F. Roy (1969), Heat flow, stress, and rate of slip along the San Andreas Fault, California, *J. Geophys. Res.*, *74*, 3821–3827.

Dibblee, T. W. (1973), Regional geologic map of the San Andreas and related faults in Carrizo Plain, Temblor, Caliente, and La Panza ranges and vicinity, California, *U.S. Geol. Surv. Misc. Geol. Invest. Map, I-757*.

Escartín, J., M. Andreani, G. Hirth, and B. Evans (2008), Relationships between the microstructural evolution and the rheology of talc at elevated pressures and temperatures, *Earth Planet. Sci. Lett.*, *268*, 463–475, doi:10.1016/j.epsl.2008.02.004.

Hardebeck, J. L., and A. J. Michael (2004), Stress orientations at intermediate angles to the San Andreas Fault, California, *J. Geophys. Res.*, *109*, B11303, doi:10.1029/2004JB003239.

Hickman, S., and M. Zoback (2004), Stress orientations and magnitudes in the SAFOD pilot hole, *Geophys. Res. Lett.*, *31*, L15S12, doi:10.1029/2004GL020043.

Hickman, S., M. Zoback, and W. Ellsworth (2004), Introduction to special section: Preparing for the San Andreas Fault Observatory at Depth, *Geophys. Res. Lett.*, *31*, L12S01, doi:10.1029/2004GL020688.

Hickman, S., M. D. Zoback, and W. L. Ellsworth (2005), Structure and composition of the San Andreas fault zone at Parkfield; initial results from SAFOD phases 1 and 2, *Eos Trans. AGU*, *86*(52), Fall Meet. Suppl., Abstract T23E-25.

Hickman, S. H., M. D. Zoback, W. Ellsworth, D. Kirschner, and D. E. Moore (2007), Structure and composition of the San Andreas Fault at seismogenic depths: Recent results from the SAFOD experiment, *Geol. Soc. Am. Abstr. Programs*, *39*, 422.

Ikari, M. J., D. M. Saffer, and C. Marone (2007), Effect of hydration state on the frictional properties of montmorillonite-based fault gouge, *J. Geophys. Res.*, *112*, B06423, doi:10.1029/2006JB004748.

Irwin, W. P., and I. Barnes (1975), Effect of geologic structure and metamorphic fluids on seismic behavior of the San Andreas Fault system in central and northern California, *Geology*, *3*, 713–716.

Kopf, A. (2007), Comparison of the mechanical properties of seismogenic fault gouge from extensional, strike-slip, and compressional fault zone drilling, *Geophys. Res. Abstr.*, *9*, Abstract EGU2007-A-05498.

Marone, C. (1998), Laboratory-derived friction laws and their application to seismic faulting, *Annu. Rev. Earth Planet Sci.*, *26*, 643–696.

Marone, C., and C. H. Scholz (1988), The depth of seismic faulting and the upper transition from stable to unstable fault regimes, *Geophys. Res. Lett.*, *15*, 621–624.

Moore, D. E., and M. J. Rymer (2007), Talc-bearing serpentinite and the creeping section of the San Andreas fault, *Nature*, *448*, 795–797, doi:10.1038/nature06064.

Morrow, C. A., and D. A. Lockner (2001), Hayward fault rocks: Porosity, density, and strength measurements, *U.S. Geol. Surv. Open File Rep., 01-421*.

Morrow, C., B. Radney, and J. Byerlee (1992), Frictional strength and the effective pressure law of montmorillonite and illite clays, in *Fault Mechanics and Transport Properties of Rocks*, *Int. Geophys. Ser.*, vol. 51, edited by B. Evans and T.-F. Wong, pp. 69–88, Academic, London.

Morrow, C. A., D. E. Moore, and D. A. Lockner (2000), The effect of mineral bond strength and adsorbed water on fault gouge frictional strength, *Geophys. Res. Lett.*, *27*, 815–818.

Morrow, C., J. Solum, S. Tembe, D. Lockner, and T.-F. Wong (2007), Using drill cutting separates to estimate the strength of narrow shear zones at SAFOD, *Geophys. Res. Lett.*, *34*, L11301, doi:10.1029/2007GL029665.

Reinen, L. A., J. D. Weeks, and T. E. Tullis (1991), The frictional behavior of serpentinite: Implications for aseismic creep on shallow, crustal faults, *Geophys. Res. Lett.*, *18*, 1921–1924.

Saffer, D. M., and C. Marone (2003), Comparison of smectite- and illite-rich gouge frictional properties: Application to the updip limit of the seismogenic zone along subduction megathrusts, *Earth Planet. Sci. Lett.*, *215, 219–235*.

Sass, J. H., C. F. Williams, A. H. Lachenbruch, S. P. Galanis Jr., and F. V. Grubb (1997), Thermal regime of the San Andreas Fault near Parkfield, California, *J. Geophys. Res.*, *102*, 27,575–27,585.

Schleicher, A. M., B. A. van der Pluijm, J. G. Solum, and L. N. Warr (2006), Origin and significance of clay-coated fractures in mudrock fragments of the SAFOD borehole (Parkfield, California), *Geophys. Res. Lett.*, *33*, L16313, doi:10.1029/2006GL026505.

Scholz, C. H. (2000), Evidence for a strong San Andreas Fault, *Geology*, *28*, 163–166.

Sims, J. D. (1988), Geologic map of the San Andreas Fault zone in the Cholame Valley and Cholame Hills quadrangles, San Luis Obispo and Monterey counties, California, *U.S. Geol. Surv. Misc. Field Stud. Map, MF-1995*.

Solum, J. G., S. H. Hickman, D. A. Lockner, D. E. Moore, B. A. van der Pluijm, A. M. Schleicher, and J. P. Evans (2006), Mineralogical characterization of protolith and fault rocks from the SAFOD Main Hole, *Geophys. Res. Lett.*, *33*, L21314, doi:10.1029/2006GL027285.

Tembe, S., D. A. Lockner, J. G. Solum, C. A. Morrow, T. Wong, and D. E. Moore (2006), Frictional strength of cuttings and core from SAFOD drillhole phases 1 and 2, *Geophys. Res. Lett.*, *33*, L23307, doi:10.1029/2006GL027626.

Thayer, M., and R. Arrowsmith (2005), Fault zone structure of Middle Mountain, central California, *Eos Trans. AGU*, *86*(52), Fall Meet. Suppl., Abstract T21A-0458.

Thayer, M. R., J. R. Arrowsmith, J. J. Young, A. K. Fayon, and M. J. Rymer (2004), Geologic structure of Middle Mountain within the San Andreas Fault zone near Parkfield, California, *Eos Trans. AGU*, *85*(47), Fall Meet. Suppl., Abstract T13A-1335.

Williams, C. F., F. V. Grubb, and S. P. Galanis Jr. (2004), Heat flow in the SAFOD pilot hole and implications for the strength of the San Andreas Fault, *Geophys. Res. Lett.*, *31*, L15S14, doi:10.1029/2003GL019352.

Zoback, M. D., et al. (1987), New evidence on the state of stress of the San Andreas Fault system, *Science*, *238*, 1105–1111.

B. M. Carpenter, C. Marone, and D. M. Saffer, Department of Geosciences and Energy Institute Center for Geomechanics, Geofluids, and Geohazards, Pennsylvania State University, 522 Deike Building, University Park, PA 16802, USA. (bcarpent@geosc.psu.edu)